Biochimica et Biophysica Acta 1837 (2014) 1522–1532

Contents lists available at ScienceDirect

Biochimica et Biophysica Acta

journal homepage: www.elsevier.com/locate/bbabio

Characterization of wave phenomena in the relaxation of flash-induced chlorophyll fluorescence yield in cyanobacteria ☆

Zsuzsanna Deák, László Sass, Éva Kiss, Imre Vass *

Institute of Plant Biology, Biological Research Centre of the Hungarian Academy of Sciences, Temesvari krt. 62, 6726 Szeged, Hungary

ARTICLE INFO

Article history:
Received 9 December 2013
Received in revised form 30 December 2013
Accepted 7 January 2014
Available online 14 January 2014

Keywords:
Photosystem II
Variable Chl fluorescence
Linear electron transport
Cyclic electron transport
NDH-1 complex

ABSTRACT

Fluorescence yield relaxation following a light pulse was studied in various cyanobacteria under aerobic and microaerobic conditions. In *Synechocystis* PCC 6803 fluorescence yield decays in a monotonous fashion under aerobic conditions. However, under microaerobic conditions the decay exhibits a wave feature showing a dip at 30–50 ms after the flash followed by a transient rise, reaching maximum at ~1 s, before decaying back to the initial level. The wave phenomenon can also be observed under aerobic conditions in cells preilluminated with continuous light. Illumination preconditions cells for the wave phenomenon transiently: for few seconds in *Synechocystis* PCC 6803, but up to one hour in *Thermosynechocystis elongatus* BP-1. The wave is eliminated by inhibition of plastoquinone binding either to the Q_B site of Photosystem-II or the Q_o site of cytochrome b_6f complex by 3-(3′,4′-dichlorophenyl)-1,1-dimethylurea or 2,5-dibromo-3-methyl-6-isopropyl-p-benzoquinone, respectively. The wave is also absent in mutants, which lack either Photosystem-I or the NAD(P)H-quinone oxidoreductase (NDH-1) complex. Monitoring the redox state of the plastoquinone pool revealed that the dip of the fluorescence wave corresponds to transient oxidation, whereas the following rise to re-reduction of the plastoquinone pool. It is concluded that the unusual wave feature of fluorescence yield relaxation reflects transient oxidation of highly reduced plastoquinone pool by Photosystem-I followed by its re-reduction from stromal components via the NDH-1 complex, which is transmitted back to the fluorescence yield modulator primary quinone electron acceptor via charge equilibria. Potential applications of the wave phenomenon in studying photosynthetic and respiratory electron transport are discussed. This article is part of a Special Issue entitled: Photosynthesis Research for Sustainability: Keys to Produce Clean Energy.

1. Introduction

Measurement of flash-induced chlorophyll (Chl) fluorescence relaxation has been proven to be a highly informative method to study the kinetics of photosynthetic electron transport processes, which lead to changes in the redox state of the Q_A primary quinone electron acceptor of Photosystem II (see Refs. [1–7]). The underlying phenomenon behind the method is the modulation of the yield of variable Chl fluorescence by the reduction state of Q_A, which leads to high fluorescence yield when Q_A is in the reduced state, and to low fluorescence yield when Q_A is in the oxidized state (see [8–10]). As a consequence, all of the electron transport processes that lead to changes in the redox state of Q_A can be monitored in a technically straightforward way by measuring Chl fluorescence yield.

Single turnover flash illumination transfers an electron from the water oxidizing complex to the first quinone electron acceptor, Q_A, which results in a prompt increase of fluorescence yield due to formation of Q_A^-. In PSII centers with functional donor and acceptor side electron transfer the flash-induced increase of fluorescence yield usually relaxes in a monotonously decreasing fashion, consisting of three main phases (see [1–6]). These phases are assigned to different pathways of Q_A^- reoxidation as discussed in [11–13]: (i) by Q_B (or Q_B^-) which is bound to the Q_B site at the time of the flash (fast phase, T_1 ~ 300–500 μs), (ii) by plastoquinone (PQ) which binds to the Q_B site after the flash (middle phase, T_2 ~ 5–15 ms), and (iii) by recombination of the electron on $Q_AQ_B^-$, via the $Q_A^-Q_B \leftrightarrow Q_AQ_B^-$ charge equilibrium, with the oxidized S_2 (or S_3) state of the water-oxidizing complex (slow phase, T_3 ~ 10–20 s). In the presence of electron transport inhibitors, which block the Q_B site, such as DCMU, the relaxation is dominated by a slow component (1–2 s), that reflects the reoxidation of Q_A^- via charge recombination with the S_2 state. When Q_B site inhibition occurs in PSII centers in which electron transfer is partly, or completely inhibited between the water oxidizing complex and Tyr-Z, that serves

Abbreviations: Chl, chlorophyll; DCMU, 3-(3′,4′-dichlorophenyl)-1,1-dimethylurea; DMBQ, 2,5-dimethyl-p-benzoquinone; DBMIB, 2,5-dibromo-3-methyl-6-isopropyl-p-benzoquinone; NDH-1, NAD(P)H-quinone oxidoreductase; PQ and PQH_2, plastoquinone and plastoquinol, respectively

☆ This article is part of a Special Issue entitled: Photosynthesis Research for Sustainability: Keys to Produce Clean Energy.

* Corresponding author. Tel.: +36 62 599 700; fax: +36 62 433 434.
E-mail address: vass.imre@brc.mta.hu (I. Vass).

0005-2728/$ – see front matter © 2014 Elsevier B.V. All rights reserved.
http://dx.doi.org/10.1016/j.bbabio.2014.01.003

as intermediate electron donor to P_{680}^{+}, Tyr-Z^{+} will be stabilized and will act as a recombination partner of Q_A^- instead of the S_2 (S_3) state leading to a fast decaying (few ms) fluorescence relaxation component [2,14].

Analysis of the fluorescence decay phases gives useful information on the kinetics of the above described electron transport processes, and makes it possible to calculate the rate of forward electron transport between Q_A and Q_B (Q_B^-), the binding rate of PQ to the Q_B site, as well as the rates of charge recombination between the S_2 state and the reduced Q_A and Q_B acceptors. In addition, it is possible to estimate the free energy (redox potential) differences between various acceptor ($Q_A \leftrightarrow Q_B$) and donor (Tyr-Z $\leftrightarrow$ S_2) components (see [1–5]). Since the method can be applied both in isolated thylakoid membrane preparations, and in intact cells it has become a widely used approach to study modifications of PSII electron transfer caused either by environmental stress effects, or by various mutations occurring naturally or produced by targeted research efforts (see Refs [1–7,15–20]). Although the dominating amount of literature data shows monotonic decay of the flash-induced fluorescence yield we have previously observed unusual wave features in the fluorescence relaxation in intact cells of the cyanobacterium *Thermosynechococcus elongatus* BP-1 (denoted as *Thermosynechococcus*) [21]. A biphasic decay of fluorescence showing a shoulder was also observed in *Synechocystis* sp. PCC 6803 (which will be denoted as *Synechocystis* hereafter) [18]. This wave phenomenon was investigated here in more detail in various cyanobacteria. The results demonstrate that wave features in the decay of flash-induced fluorescence yield represent a general phenomenon that reflects transient changes in the reduction level of the PQ pool due to imbalance between the different electron transport pathways of the thylakoid membrane.

2. Materials and methods

2.1. Culture conditions

Synechocystis and *Synechococcus* sp. PCC 7942 (denoted as *Synechococcus* hereafter) cells were grown in BG-11 medium on a rotary shaker under continuous illumination of 40 μmol photons m^{-2} s^{-1} intensity white light at constant temperature of 30 °C, supplied by 3% CO_2. The M55 (ΔndhB) mutant of *Synechocystis* [22] was a kind gift of Dr. Teruo Ogawa, and was grown under the same conditions as the WT in BG-11 medium supplemented with kanamycin (20 μg mL^{-1}). The PSI-less (Δ*psaAB*) mutant obtained from the laboratory of Prof. Vermaas [23] was grown under 5 μmol photons m^{-2} s^{-1} light intensity in BG-11 medium supplemented with glucose (10 mM) and chloramphenicol (25 μg mL^{-1}). High NDH-1 activity of the WT cells was achieved by growing the cultures under higher light intensity of 60–80 μmol photons m^{-2} s^{-1}, without extra CO_2 supply. Unless stated otherwise, cells used for measurements were grown under white light illumination of 40 μmol photons m^{-2} s^{-1} and the growing chamber was supplied by 3% CO_2.

Thermosynechococcus elongatus BP-1 cells were routinely grown in BG-11 medium in a rotary shaker at 40 °C under 0.1% CO_2 atmosphere. The intensity of the illumination was 40 μmol photons m^{-2} s^{-1}. For freeze–thaw treatment cells were kept at −80 °C for 2 h, then thawed on ice and kept at room temperature for 2 h in the dark. Thylakoids from *Thermosynechococcus* were isolated as in [15], and were a kind gift from the laboratory of Prof. James Barber. Chl concentration of the thylakoids was 10 μg mL^{-1}.

Acaryochloris marina MBIC11017 (denoted as *Acaryochloris*) cells were obtained from the laboratory of Dr. Min Chen and were grown in artificial sea water plus iron (4 mg L^{-1}) at 6–10 μmol photons m^{-2} s^{-1}, at 27 °C in conical flasks during continuous shaking. For measurements cells were harvested in their late exponential growth phase. After centrifugation (4000 ×*g* for 10 min) cells were resuspended in fresh culture medium to achieve final Chl concentration of 5 μg mL^{-1}.

2.2. Microaerobic conditions

Microaerobic conditions were achieved by the addition of glucose, glucose oxidase (Sigma) and catalase (Sigma) at final concentration of 10 mM, 7 U mL^{-1} and 60 U mL^{-1}, respectively. Under our experimental conditions oxygen content of the sample dropped below 1 μmol L^{-1} within 3 min as monitored with an immersible fiber-optic oxygen meter (Fibox 3, Presens).

2.3. Flash-induced increase and subsequent decay of chlorophyll fluorescence yield

Flash-induced increase and subsequent decay of chlorophyll fluorescence yield was measured using a double-modulation fluorometer (FL-3000, Photon System Instruments, Brno) [24]. For measurements cells were harvested in their late exponential growth phase. After centrifugation (4000 ×*g* for 10 min) cells were resuspended in fresh culture medium to achieve final Chl concentration of 5 μg mL^{-1}. The instruments LED system provides both single turnover saturating actinic flashes (20 μs, 639 nm) and measuring flashes (8 μs, 620 nm). Fluorescence decay was recorded in the 150 μs to 100 s time range on a logarithmic time scale. Flash-induced fluorescence relaxation curves were analyzed as described by [2]. Multicomponent deconvolution of the monotonically decreasing curves was done by using a fitting function with two exponential components (fast and middle phase) and one hyperbolic component (slow phase):

$$F_{v,corr} = A_1 \exp(-t/T_1) + A_2 \exp(-t/T_2) + A_3/(1 + t/T_3) + A_0$$

where $F_v = F(t) - Fo$, F(t) is the fluorescence yield at time t, Fo is the basic fluorescence level before the flash, A_1–A_3 are the amplitudes, and T_1–T_3 are the time constants. Non decaying fluorescence component in the time span of the measurement is described by a constant A_0 amplitude. $F_{v,corr}$ is the variable fluorescence yield corrected for non-linearity, taking into consideration the nonlinear correlation between fluorescence yield and the redox state of Q_A using the Joliot model [25], with a value of 0.5 for the energy-transfer parameters between PSII units.

2.4. Post-illumination rise of the fluorescence yield

Post-illumination rise of the fluorescence yield [26] was measured by a double-modulation fluorometer (FL-3000, Photon System Instruments, Brno). Continuous red (639 nm) actinic illumination was applied for 30 s corresponding to the growth light intensity of the examined cells followed by a dark period. Fluorescence was detected by weak measuring flashes (8 μs, 620 nm) at every 1 s in the last 5 s of the illumination period, then every 50 ms in the first 2 s of the dark period, followed by 0.5 s repetition rate of measuring flashes in the remaining time of dark adaptation.

2.5. Simulation of fluorescence traces

Simulation of fluorescence traces was performed by using a mathematical model of electron transport processes on the basis of an electron transport network, which is shown in Scheme 1. The model includes 52 electron transport processes, which are listed in Supplementary Table 1. These processes are described by a set of connected linear differential equations according to the topology shown in Scheme 1, and solved numerically using the Matlab software package. The rate constants of the forward and backward electron transport processes (shown in Supplementary Table 2) were taken from the literature, or obtained from our own measurements. When data were not available for the backward rates we used the reasonable estimation that the reverse processes proceed with 5–10% rate of the forward processes.

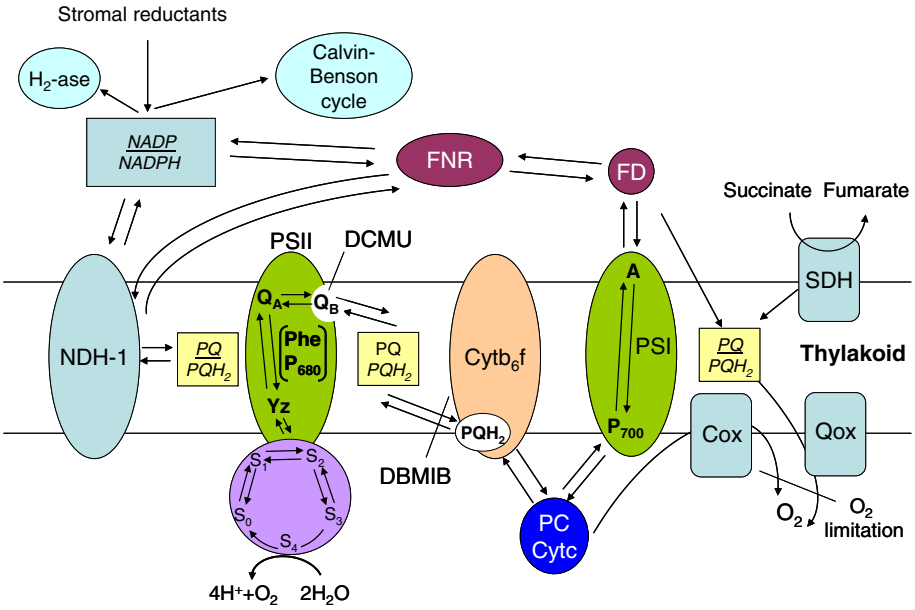

Scheme 1. Schematic representation of the photosynthetic and respiratory electron transport pathways in cyanobacteria. The initial step of linear electron transport is charge separation between P_{680}^{+} and Phe^{-}, and the first steps of charge stabilization occur at the reduction of Q_A and the oxidation of Tyr-Z (Y_Z). For the sake of simplicity we describe only the formation of the $Y_Z^{+}Q_A^{-}$ state. The electrons from Q_A^{-} are transferred to plastoquinone molecules (PQ) that bind to the so called Q_B site, and released to the lipid phase of the membrane after taking up 2 electrons and 2 protons (PQH_2). The PQH_2 molecules are reoxidized by the $cytb_6f$ complex, which transfers electrons to a soluble electron carrier in the thylakoid lumen. For the sake of simplicity the fine details of electron transport inside the $cytb_6f$ complex, such as the so called Q cycle are ignored. The electron carrier, which takes up electrons from $cytb_6f$ is usually plastocyanin (PC), which is a copper containing protein. However, in cyanobacteria cyt-c553 can be an alternative of PC depending on environmental conditions, such as the availability of copper. Either of these soluble electron carriers can reduce the oxidized PSI reaction center Chl $P700^{+}$, or transfer electrons to the cytochrome oxidase (Cox), which use oxygen as electron acceptor. In the PSI complex $P700^{+}$ is formed via light induced charge separation in which the electron is transferred through a series of acceptor molecules (A_0, A_1, F_X, F_A, F_B), which are considered here for the sake of simplicity as one acceptor state (A) that stabilizes the electron arriving from P700. The electrons arriving at the acceptor side of PSI transferred to ferredoxin, which is a soluble iron–sulfur protein (FD). The main route of electrons from FD is towards ferredoxin-NADP-oxidoreductase (FNR). However electrons can also be cycled back to the PQ pool via a process whose details are not well understood. The electrons arriving at FNR are utilized in the reduction of $NAD(P)^{+}$ to NAD(P)H, which is used in the Calvin cycle, in H_2 production, and can also be transferred back to the PQ pool via the NDH-1 complex. FNR can probably also transfer electrons directly to the NDH-1 complex [62]. Electrons are also fed into the PQ pool from respiration via the succinate dehydrogenase (SDH) complex. The linear electron transport pathway goes from water to the Calvin–Benson cycle, whereas the cyclic electron transport pathway proceeds via the direct Fd-dependent and the NDH-1 dependent routes.

3. Results

3.1. Microaerobic conditions induce wave phenomena in fluorescence yield relaxation in Synechocystis

A representative flash-induced Chl fluorescence decay curve of *Synechocystis* cells is shown in Fig. 1. When measured under aerobic conditions the fluorescence yield monotonically decreases in the 150 μs–100 s detection time window (Fig. 1. open circles) as reported several times in the literature [1–7,15–20]. The relaxation is dominated by the fast phase (T_1 ~ 570 μs, relative amp. 65%, Table 1), which reflects electron transfer from Q_A^{-} to Q_B (Q_B^{-}). The middle phase (6 ms, 18%) arises from reoxidation of Q_A^{-} by PQ which binds to the Q_B site after flash, whereas the slow phase (10 s, 17%), arises from the $S_2Q_AQ_B^{-}$ charge recombination (see [2]). However, an unusual behavior of fluorescence relaxation is observed when the cells are kept under microaerobiosis (corresponding to < 0.3% of the oxygen content of aerated samples with ~300 μmol L^{-1} dissolved oxygen). Under such conditions the initial phase of the decay (up to 20 ms after the flash) becomes significantly slower than in the aerated samples (Fig. 1. closed circles). In addition, the curve shows a transient drop reaching a minimum value of the fluorescence yield at around 30–50 ms after the flash (denoted as "dip"), followed by an overshoot (denoted as "bump") with maximal intensity at around 1 s (Fig. 1, closed circles) leading to a wave feature in the relaxation. In order to see clearly the changes in the relaxation kinetics under different experimental conditions the fluorescence decay kinetics are usually shown in the figures after shifting the Fo level of the curves to 0, and normalization of the initial amplitudes to 1. It has to be noted however, that oxygen deprivation leads also to the increase of the Fo level as shown by the fluorescence relaxation curves in the inset. The elevated Fo level shows that the PQ pool becomes highly reduced in the microaerobic samples after the 15 min dark period, which is applied before the flash illumination.

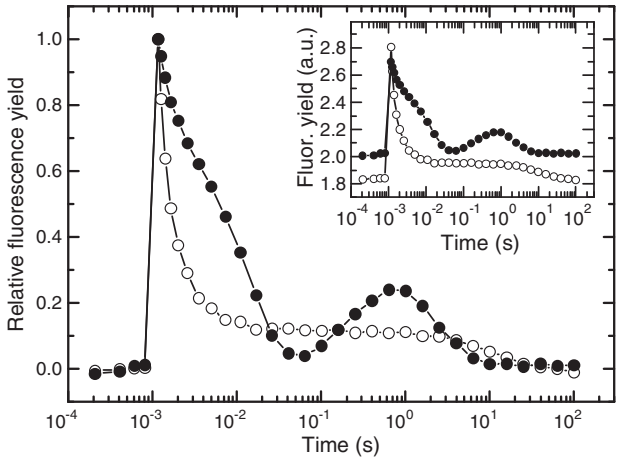

Fig. 1. Flash-induced fluorescence yield changes in *Synechocystis* cells. Relaxation curves were detected after 3 min dark adaptation at room temperature (open circles) and after 15 min microaerobic incubation (closed circles) achieved by the addition of 10 mM glucose, 7 U mL^{-1} glucose oxidase and 60 U mL^{-1} catalase. Curves were normalized to the same initial amplitudes. The insert shows the original curves without normalization.

To investigate the origin of the wave feature in the fluorescence yield during relaxation various electron transport inhibitors and acceptors were applied. When the Q_A to Q_B electron transport step is blocked by DCMU (Scheme 1), the dominating phase of fluorescence relaxation in the aerobic samples is slowed down (1 s), which reflects Q_A^{-} reoxidation via the $S_2Q_A^{-}$ charge recombination (Fig. 2A, closed squares).

Table 1
Decay kinetics of flash-induced variable fluorescence in *Synechocystis* cells under aerobic and microaerobic conditions in the presence of electron transport inhibitors and acceptors. Multicomponent deconvolution of the fluorescence relaxation curves presented in Fig. 2. The kinetics were analyzed in terms of two exponential components (fast and middle phase) one hyperbolic component (slow phase) and a nondecaying component as described in Materials and methods. Values after slash are relative amplitudes as a percentage of total variable yield. Standard errors of the calculated parameters are also indicated.

	Fast phase T_1(μs)/A_1(%)	Middle phase T_2(ms)/A_2(%)	Slow phase T_3(s)/A_3(%)	Nondecaying phase A_0 (%)
Aerobic conditions				
No addition	570 ± 50/65.1 ± 2.5	6.2 ± 1.3/17.7 ± 2.6	10.3 ± 1.3/17.3 ± 0.4	0
+DCMU	–/0	–/0	1.0 ± 0.1/100 ± 0.5	0
+DBMIB	770 ± 80/52.2 ± 2.3	22.8 ± 3.4/27.1 ± 1.7	6.1 ± 1.1/20.7 ± 0.8	0
+DMBQ	430 ± 50/53.7 ± 3.1	12.1 ± 2.1/20.9 ± 1.6	17.8 ± 2.1/25.4 ± 0.5	0
Microaerobic conditions				
+DCMU	–/0	0.9 ± 0.2/1.9 ± 0.4	1.1 ± 0.1/94.2 ± 1.0	3.9 ± 0.8
+DBMIB	2480 ± 500/16.9 ± 3.3	33.2 ± 9.7/23.9 ± 3.3	1.4 ± 0.1/59.2 ± 1.8	0
+DMBQ	680 ± 80/55.6 ± 2.6	16.1 ± 3.3/21.4 ± 2.0	9.1 ± 2.6/20.1 ± 1.5	2.9 ± 0.6

Importantly, the above described wave in the fluorescence yield decay observed in oxygen deprived cultures (Fig. 2B open circles) was completely abolished by the addition of DCMU (Fig. 2B, closed squares).

Another electron transport inhibitor, DBMIB, binds to the Q_o pocket of the cytochrome (cyt) b_6f complex [27] and blocks PQ oxidation at this site (Scheme 1) leading to the accumulation of reduced PQ (PQH_2) in the thylakoid membrane. In the presence of DBMIB the relative amplitude of the middle phase of fluorescence relaxation is increased (27%) at the expense of the fast phase in the aerobic samples (Fig. 2A closed diamonds, Table 1). This effect can be explained by the decreased amount of bound PQ at the Q_B site due to higher number of reduced PQ molecules (PQH_2) in the thylakoid membrane. Importantly, DBMIB inhibits the development of the wave in flash-induced fluorescence decay caused by oxygen deprivation (Fig. 2B, closed diamonds). The dominating decay component in this case is the slow phase (59%), indicating the accumulation of Q_A^- in the same fraction of centers, which are reoxidized by charge recombination with S_2 state (Table 1). DMBQ, a lipid soluble and stable electron acceptor of PSII [28], which keeps the PQ pool largely oxidized, slightly increases the relative amplitudes as well as the time constants of the middle and the slow phases of fluorescence decay under aerobic conditions (Fig. 2A closed triangles, Table 1). Under microaerobic conditions the presence of DMBQ also abolished the wave in the fluorescence yield (Fig. 2B, closed triangles).

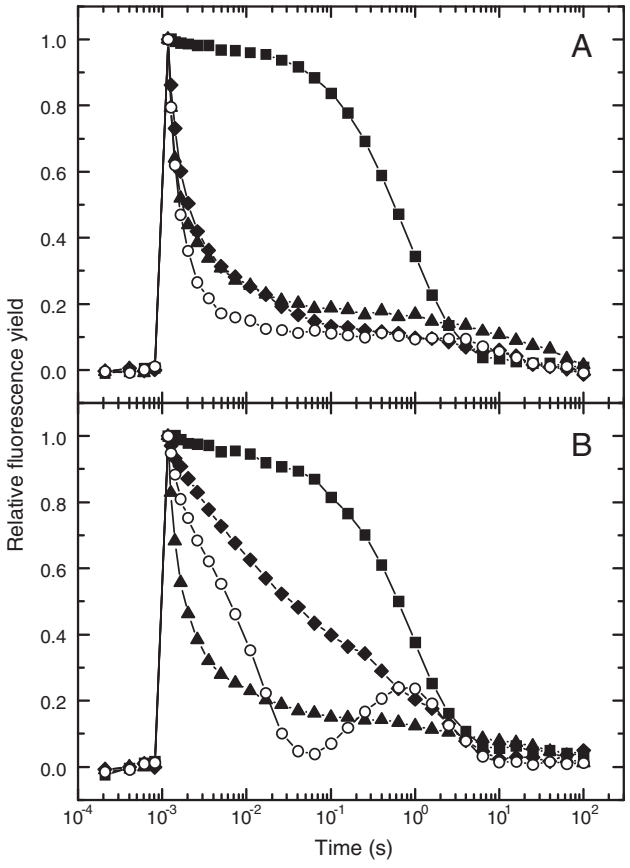

Fig. 2. Effect of electron transport inhibitors and electron acceptors on flash-induced fluorescence yield changes in *Synechocystis* cells. Relaxation curves were detected after 3 min dark adaptation (A), and after 15 min microaerobic incubation (B) achieved by the addition of 10 mM glucose, 7 U mL^{-1} glucose oxidase and 60 U mL^{-1} catalase. Electron transport inhibitors and acceptors were added 2 min before the measurements: 10 μM DCMU (squares), 5 μM DBMIB (diamonds), 0.5 mM DMBQ (triangles), no addition (circles). The curves were normalized to the same initial amplitudes.

The above described effects of DCMU, DBMIB and DMBQ on the kinetics of fluorescence relaxation under microaerobic conditions demonstrate that the reduction state of the PQ pool, together with free electron transport through it play a crucial role in the wave feature of the Chl fluorescence yield relaxation.

3.2. The NDH-1 complex and PSI are both required for the waving fluorescence yield relaxation in Synechocystis

PSI-mediated cyclic electron transport removes electrons from the PQ pool via the $cytb_6f$ complex and plastocyanin (PC) or cyt-c553, and also feeds electrons back to the pool via the thylakoid bound NAD(P)H-quinone oxidoreductase complex (NDH-1) (see [29]) (Scheme 1). The possible role of NDH-1 and PSI complexes in the fluorescence wave phenomenon can be conveniently studied by mutants lacking a functional form of these complexes. Under aerobic conditions relaxation of flash-induced fluorescence yield in the M55 mutant, which lacks the B subunit of the NDH-1 complex [30] is almost the same as in the WT (Fig. 3A open triangles), and the time constants and relative amplitudes of the three decay phases are also very similar in the two strains (Table 2.). In the PSI-less strain the relaxation is very similar to that in the WT although the relative amplitude of the middle phase is increased (by 8%) at the expense of the fast phase (Table 2.), indicating an increased reduction level of the PQ pool in the absence of PSI.

Under microaerobic conditions the flash-induced fluorescence relaxation kinetics are significantly different in the mutant and WT strains. In contrast to the wave behavior seen in the WT (Fig. 1) no such phenomenon was observed in the fluorescence decay curve of either the M55, or the PSI-less strain when the oxygen content of the media was decreased (Fig. 3A and B, closed symbols). In the M55 mutant the time constant and the relative amplitude of the middle phase increased to a small extent, while the amplitude of the fast phase decreased (Table 2, Fig. 3A, closed triangles). In the PSI-less mutant the fluorescence decay curve is dominated by the slow phase (81%),

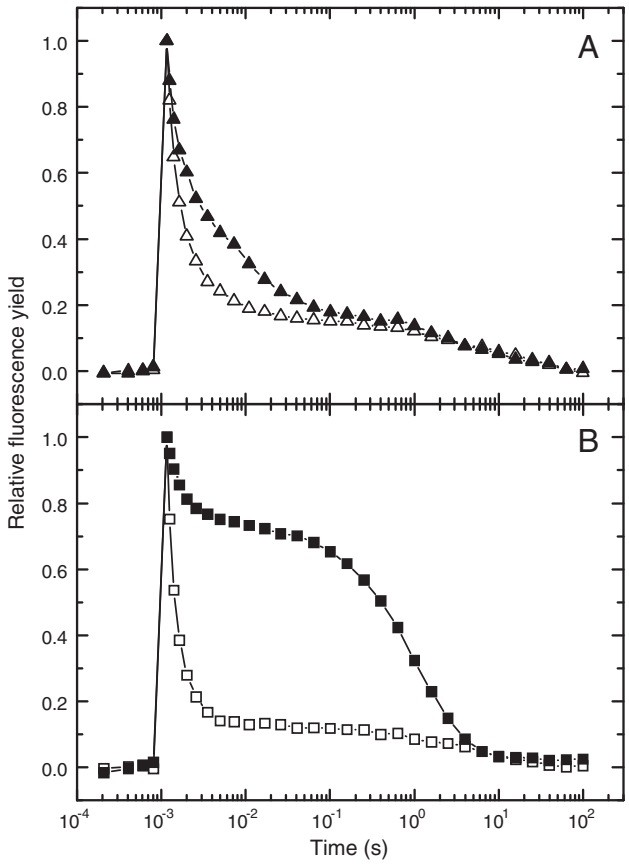

Fig. 3. The effect of lacking the NDH-1 complex, or PSI on flash-induced fluorescence yield changes in *Synechocystis* cells. The kinetics of fluorescence decay is shown for the NDH1-less M55 (A) and PSI-less (B) mutant cells. Relaxation curves were measured after 3 min dark adaptation (open symbols), and after 15 min microaerobic incubation (closed symbols) achieved by the addition of 10 mM glucose, 7 U mL^{-1} glucose oxidase and 60 U mL^{-1} catalase. Curves were normalized to the same initial amplitudes.

showing a large extent of reduction of the PQ pool (Fig. 3B, closed squares). The time constant of this decay phase (1.2 s, Table 2.) shows that Q_A^- reoxidation occurs mostly via charge recombination with stable PSII donor(s) ($S_2Q_A^-$) in the oxygen deprived PSI-less mutant.

The above results show that both the PSI and NDH-1 complexes are required for the appearance of the waving yield of flash-induced Chl fluorescence, and point to the involvement of alternative electron transport pathway(s) around PSI in the wave phenomenon.

3.3. High reduction level of the PQ pool is required for waving fluorescence yield relaxation in Synechocystis

In order to obtain further insight into the mechanism of fluorescence yield wave we were searching for experimental conditions in which the reduction state of the PQ pool increases significantly even under aerobic conditions while intact electron flow through PSII and PSI is maintained. Such a situation can be found under conditions, which induce transient reduction of the PQ pool by NDH-1 mediated electron flow in darkness, and lead to the so called post-illumination rise in Chl fluorescence [26,31–36]. The activity of the NDH-1 complex in cyanobacterial cells alters at different growth phases [37] and can also be affected by various factors, such as CO_2 concentration [38,39], light, and temperature [40,41]. In our laboratory *Synechocystis* is cultured at 30 °C, 40 μmol photons m^{-2} s^{-1} light intensity, and CO_2 enriched (3%) atmosphere. When cells grown under these conditions were illuminated by growth light intensity for 30 s they showed only negligible post-illumination rise of Chl fluorescence yield (Fig. 4A, dotted line). However when cells were grown under atmospheric CO_2 and elevated light intensity (60 μmol photons m^{-2} s^{-1}) a significant increase of fluorescence yield was observed after switching off the actinic illumination (Fig. 4A, solid line). This fluorescence rise shows a rapid reduction of the PQ pool in darkness that reaches maximal level after a ~1 s dark period. We checked the relaxation kinetics of flash-induced fluorescence yield at the time of maximal PQ pool reduction, i.e. in a sample preilluminated for 30 s by growth light followed by 1 s dark interval as indicated by the arrow in Fig. 4A. However, fluorescence relaxation measured in this way is influenced by the significantly changing yield of post-illumination fluorescence rise superimposed on the flash-induced change of the fluorescence yield. In order to compensate for the change of the background signal a baseline curve was measured without any flash excitation and subtracted from the flash induced trace. The resulting curve shows a pronounced wave in flash-induced fluorescence yield (Fig. 4B, closed circles) supporting the idea that high reduction level of the PQ pool is required for the wave phenomenon. When the same type of measurement was performed with cells grown under normal growth conditions, which do not show the transient reduction of the PQ pool in the dark, the wave feature of the fluorescence decay was not observed (Fig. 4B, open squares).

Flash-induced fluorescence relaxation was also measured by the usual method (i.e. after 3 min dark adaptation), in cells grown at high light under atmospheric CO_2. However, in this case the fluorescence relaxation showed only the well-known monotonically decreasing kinetics (Fig. 4C, closed diamonds), which was almost identical with that observed in cells grown under the usual conditions, i.e. low light and elevated CO_2 (Fig. 4C, open triangles).

3.4. Wave feature of fluorescence yield relaxation occurs in several species of cyanobacteria

The effect of oxygen deprivation on the relaxation kinetics of flash-induced fluorescence yield was tested in different cyanobacterial species. The waving yield was induced by microaerobic incubation to a significant extent in *Synechococcus* cells (Fig. 5A, closed squares). However in the marine cyanobacterium *Acaryochloris* only the increase of the middle phase could be observed, but no clear dip or bump appeared in the fluorescence decay kinetics (Fig. 5B, closed triangles). In the

Table 2
Decay kinetics of flash-induced variable fluorescence in M55 and PSI-less *Synechocystis* mutant cells under aerobic and microaerobic conditions. Multicomponent deconvolution of the fluorescence relaxation curves presented in Fig. 3. The kinetics were analyzed in terms of two exponential components (fast and middle phase) and one hyperbolic component (slow phase) as described in Materials and methods. Values after slash are relative amplitudes as a percentage of total variable yield. Standard errors of the calculated parameters are also indicated.

	Fast phase T_1(μs)/A_1(%)	Middle phase T_2(ms)/A_2(%)	Slow phase T_3(s)/A_3(%)
M55 mutant			
Aerobic	540 ± 50/58.2 ± 2.2	7.5 ± 1.3/19.3 ± 2.0	5.7 ± 0.6/22.5 ± 0.5
Microaerobic	630 ± 80/37.2 ± 1.9	15.7 ± 1.5/34.4 ± 1.4	3.9 ± 0.4/28.4 ± 0.6
PSI-less mutant			
Aerobic	300 ± 60/57.9 ± 6.2	1.6 ± 0.4/26.0 ± 5.2	3.7 ± 0.5/16.1 ± 0.4
Microaerobic	330 ± 70/11.5 ± 2.3	1.2 ± 0.3/7.3 ± 1.5	1.2 ± 0.1/81.2 ± 0.6

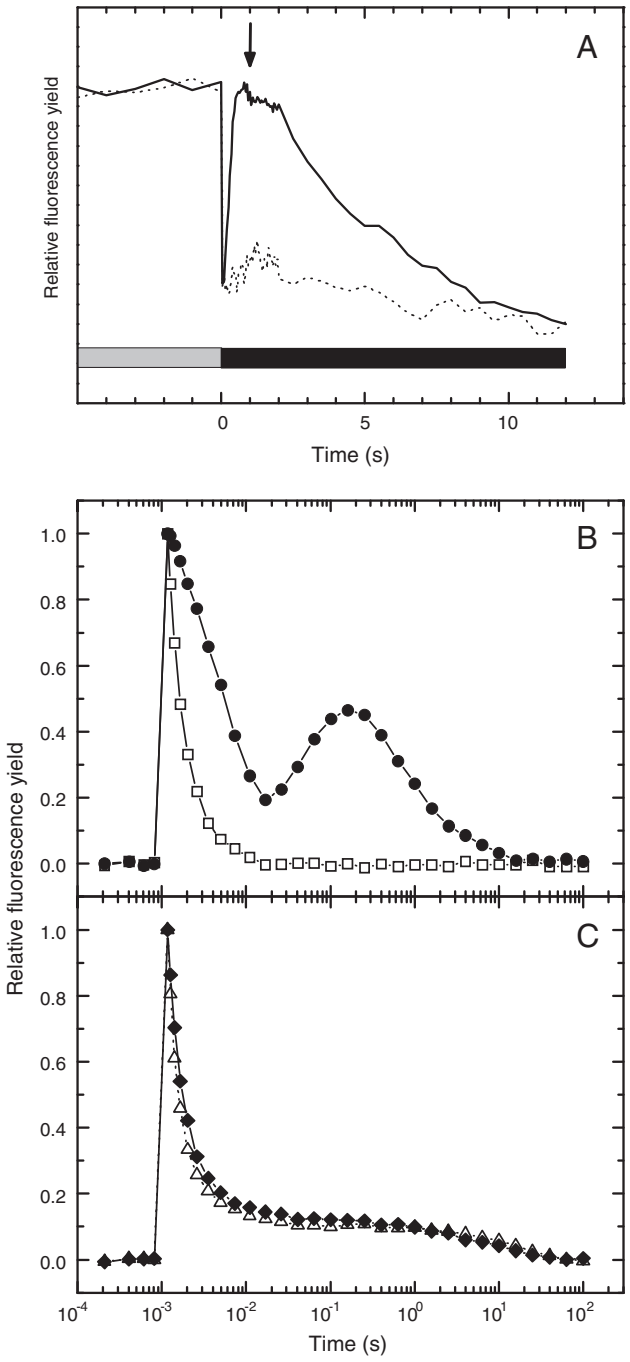

Fig. 4. Flash induced fluorescence yield changes in *Synechocystis* cells grown under different environmental conditions. Post-illumination rise of fluorescence yield (A) after 30 s illumination by growth light intensity in cells grown at 3% CO_2, 40 μmol photons m^{-2} s^{-1} light intensity (solid line) and at 0.1% CO_2, 60 μmol photons m^{-2} s^{-1} light intensity (dotted line). Growth temperature was 30 °C in both cases. Light gray bar represents the last 5 s of illumination, while dark period starts at 0 s of the scale and it is illustrated by black bar. The arrow indicates the 1 s dark point, where the exciting flash was fired in the experiments presented on panel B. Fluorescence yield changes induced by flash excitation after 1 s (B) and 3 min (C) dark time period following the 30 s growth light illumination are shown in the cells grown at 0.1% CO_2, 60 μmol photons m^{-2} s^{-1} light intensity (closed symbols) and in the cells grown at 3% CO_2, 40 μmol photons m^{-2} s^{-1} light intensity (open symbols). Curves on panel B were corrected by the background signal detected without any flash excitation. Relaxation curves were normalized to the same initial amplitudes.

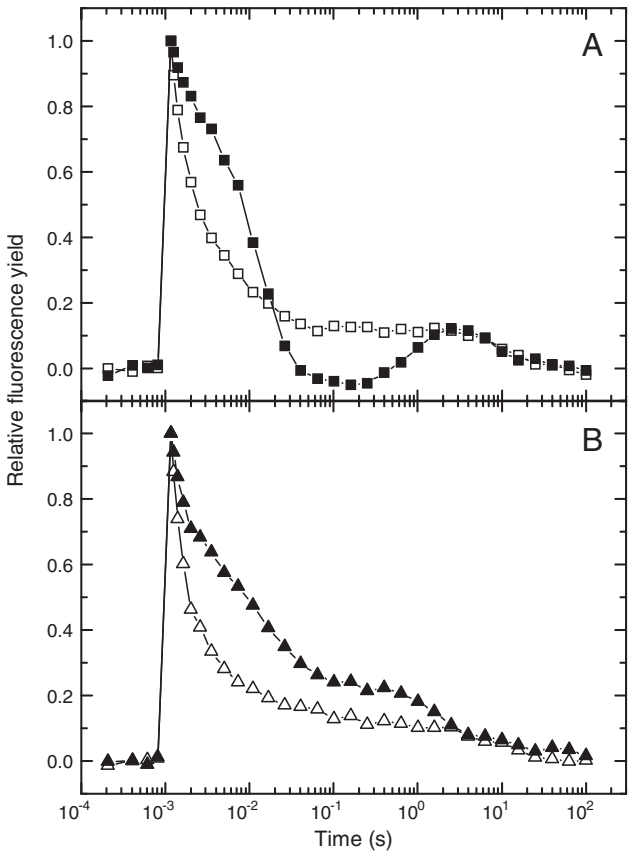

Fig. 5. Flash-induced fluorescence relaxation curves in *Synechococcus* 7942 (A) and *Acaryochloris marina* (B). Cells were grown under normal conditions (3% CO_2, 40 μmol photons m^{-2} s^{-1}) and flash-induced fluorescence yield was measured after 3 min dark adaptation in normal air (open symbols), or after 15 min incubation under microaerobic conditions (closed symbols). All curves were normalized to the same initial amplitudes.

case of the thermophilic cyanobacterium *Thermosynechococcus* unique properties of fluorescence relaxation kinetics were observed. In cultures, which were grown under low CO_2 (0.1%) post-illumination rise of fluorescence did not decay in the seconds time scale, as it was observed in the case of *Synechocystis*, but remained for several minutes at the level detected under illumination by growth light intensity (Fig. 6A). The sustained high level of post-illumination fluorescence, which decayed only after hours of dark adaptation (not shown), indicates sustained reduction of the PQ pool in the dark following an illumination period. This phenomenon was accompanied by a significant wave in the flash-induced fluorescence relaxation curve when measured in aerated samples after 3 min dark adaptation either at room temperature (Fig. 6B, closed circles), or at growth temperature (Fig. 6B, open circles). This result shows that the observed phenomenon was not caused by the shift between culturing and measuring temperatures, and the wave feature in the yield of flash-induced fluorescence occurs also under physiological conditions in intact cells of *Thermosynechococcus*.

Intactness of the cells is necessary for the appearance of the wave feature in flash-induced fluorescence decay. *Thermosynechococcus* cells previously exposed to freezing temperature (−80 °C for 2 h) do not show the wave feature (Fig. 6B, open triangles) and their decay curves are similar to ones obtained in isolated thylakoid membranes (data not shown). When cells were grown at high CO_2 (1%) the size of the wave was smaller than in the low CO_2 (0.1%) cells when measured after 3 min dark adaptation (Fig. 6C, open squares), and completely disappeared when measured after 30 min dark adaptation (Fig. 6C, closed squares).

3.5. The wave feature of fluorescence yield relaxation reflects changes in the reduction level of the PQ pool

The yield of the Chl fluorescence is modulated by the redox state of Q_A, which is influenced directly by the redox state of the PQ pool via

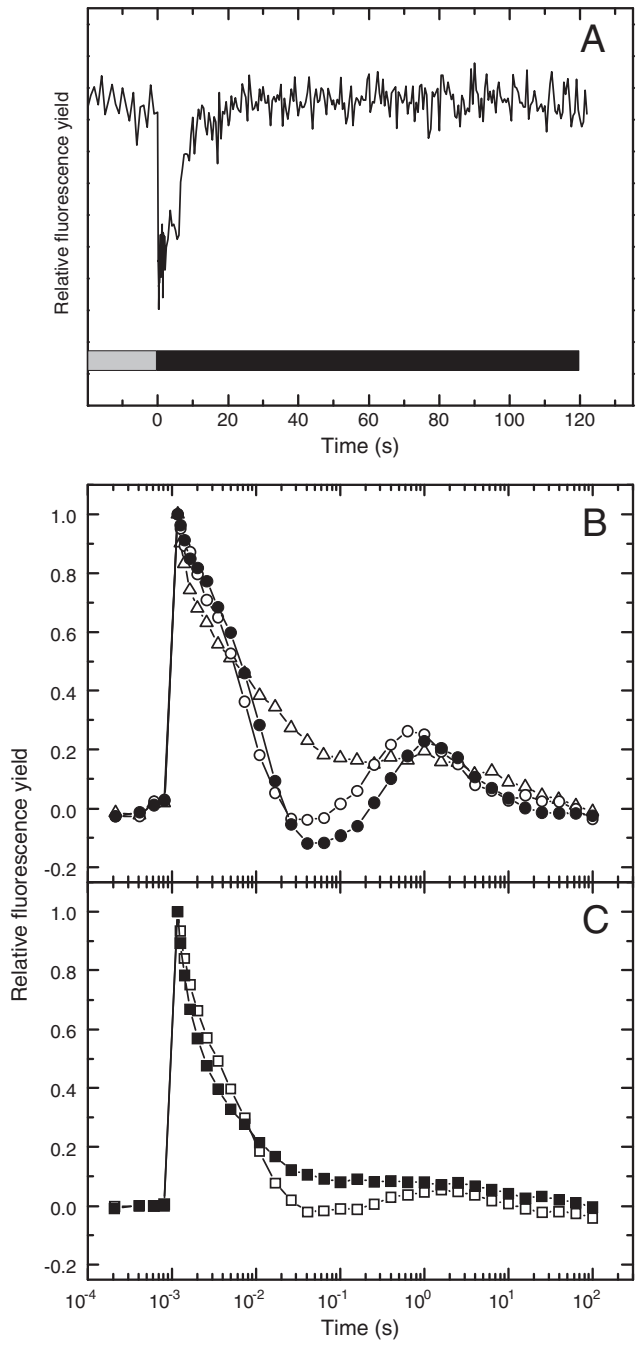

Fig. 6. Flash induced fluorescence yield changes in *Thermosynechococcus elongatus*. Cells were grown at 40 μmol photons m^{-2} s^{-1} light intensity and 40 °C temperature and either 0.1% (A, B), or 1% CO_2 (C). (A) Post-illumination rise of fluorescence yield after 30 s illumination by growth light intensity. Gray bar represents the last 20 s of preillumination, while the dark period starts at 0 s of the scale and it is illustrated by black bar. (B) Flash-induced fluorescence yield changes measured at 28 °C (solid circles) and at 40 °C growth temperature (empty circles) from intact cells grown at 0.1% CO_2, as well as in previously frozen cells (triangles). (C) Fluorescence yield changes measured at room temperature in intact cells grown at 1% CO_2. The curves were detected after 3 min (open squares) and 30 min (closed squares) dark adaptation time and were normalized to the same initial amplitudes.

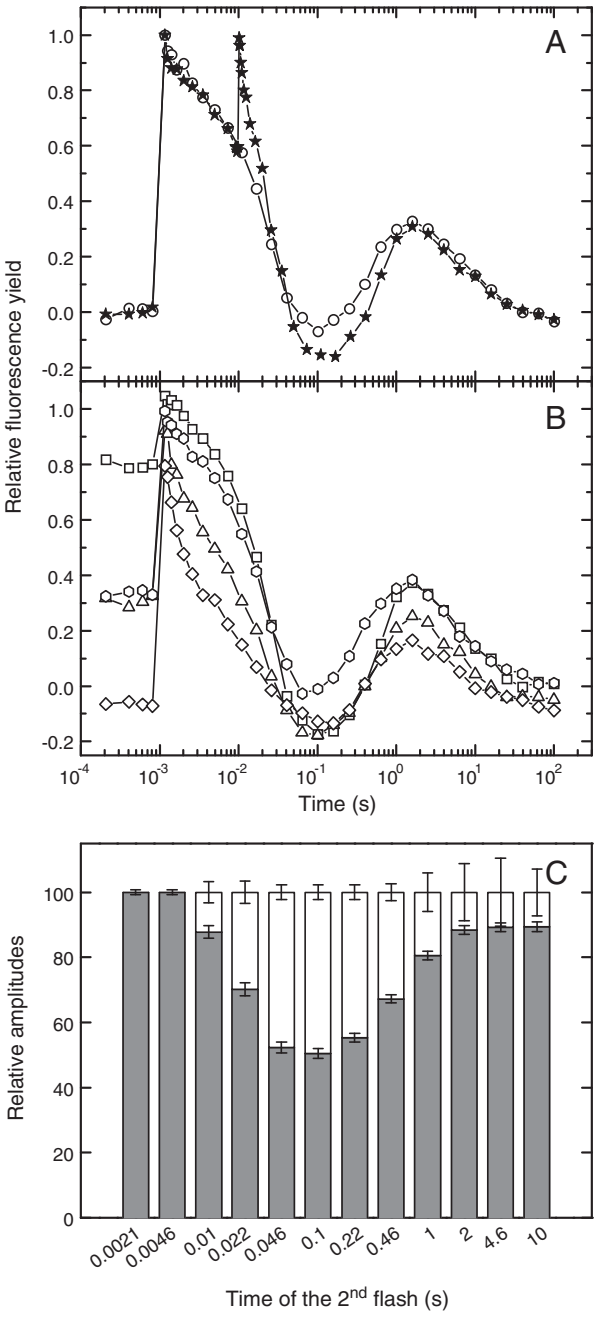

Fig. 7. Double flash experiment in *Thermosynechococcus elongatus* cells. In a standard flash-induced fluorescence measurement the single saturating flash excitation occurs at 1 ms. In double flash experiment the second saturating flash was applied at the indicated time points. An example of single (circles) and double (stars) flash-induced fluorescence yield measurement (A). In the latter case the second flash was fired at 0.01 s. Second flash induced changes were detected by the same logarithmic timing protocol as for the standard single flash decay. Second flash-induced fluorescence yield changes are shown in logarithmic time scale (B) and represent the second flash excitation at 0.0046 s (squares), 0.022 s (triangles), 0.1 s (diamonds) and 2 s (hexagon). Curves were normalized to the same initial amplitudes of the first flash induced yields. Decaying part (1 ms–100 ms) of the second flash induced curves were fitted by two exponential decay phases and the relative amplitudes of the fast (white column) and middle (gray column) phase are presented (C). The sum of the relative amplitudes was normalized to 100. Standard errors of the calculated parameters are represented by error bars. The time points of the second flash excitations are indicated on X axis.

charge equilibria through the Q_B acceptor. Therefore, the observed wave features in the fluorescence yield are expected to reflect changes in the redox state of the PQ pool. In order to obtain experimental support for this hypothesis the following measuring protocol was applied for *Thermosynechococcus* cells, which were grown at low CO_2 (0.1%) conditions. After the first actinic flash a second flash was fired with a certain time delay to probe the actual redox state of the PQ pool. An example of such a double flash experiment is shown in Fig. 7A (stars), where the second flash was given 10 ms after the first one. By changing the delay between the 1st and 2nd flashes the whole wave pattern was scanned from 1 ms up to 10 s. Fluorescence relaxation after the second

flash was detected also in the logarithmic time scale and characteristic traces, which were obtained after different time delays are presented in Fig. 7B. The first two phases of the relaxation curves – from the maximum level to the bottom of the fluorescence dip – were fitted by two exponential decay components. The relative amplitudes of the fast (white column) and middle phases (gray column) are presented in Fig. 7C. Few milliseconds after the first flash the fast phase is completely missing, and the fluorescence decay is dominated exclusively by the middle phase (Fig. 7B, squares). The fast phase was induced only after 10 ms. At longer delay times the fast phase was further increased with concomitant decrease of the middle phase, which reached its maximum after 100 ms, when the fluorescence trace has its dip (Fig. 7B, diamonds). At longer delay times the fast phase decreases again (Fig. 7B, hexagons) with concomitant increase of the relative amplitude of the middle phase (Fig. 7C).

The fast and middle phase of the fluorescence decay reflects Q_A^- re-oxidation by forward electron transport in those PSII centers, where the Q_B binding pocket is occupied or empty, respectively, at the time of the excitation flash (see [11–13]). If the fluorescence relaxation after the second flash contains only the middle phase it shows that at the time of the second flash all Q_B binding pockets were empty or occupied by PQH_2, which could be explained by the significant reduction of the PQ pool. Based on these considerations the relative amplitude of the middle phase of the fluorescence decay measured after the second flash is an indicator of the reduction level of the PQ pool. Consequently, Fig. 7C shows that right after the flash the PQ pool is extensively reduced, then it becomes partially oxidized, reaching maximal level of oxidation at the time of the dip of the fluorescence trace (ca. 100 ms), and re-reduced again after longer periods of time.

The role of PQ pool reduction in the formation of the bump feature of the fluorescence yield wave could be further verified by the following experiment. Fluorescence was detected in a control experiment by a series of measuring flashes placed on a logarithmic time scale resulting in the usual wave feature (Fig. 8 empty circles). Alternatively, from the position of the bottom of the dip (100 ms) a linear sequence of closely spaced (2 ms) measuring flashes were applied (Fig. 8, solid line). This protocol resulted in weak illumination from the time point of the dip leading to oxidation of the PQ pool due to PSI activity, and consequently to the disappearance of the bump from the fluorescence relaxation kinetics (Fig. 8, solid line).

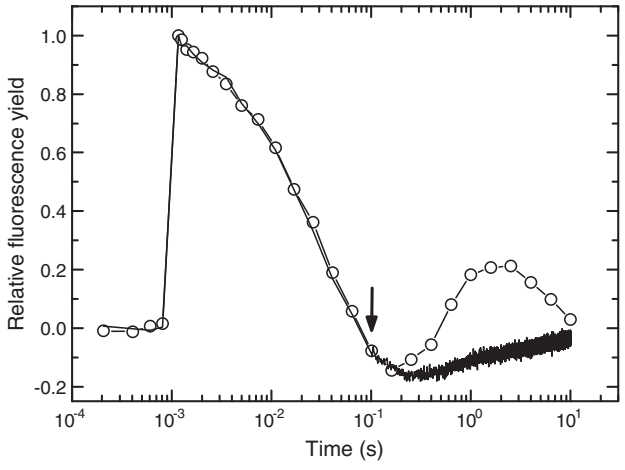

Fig. 8. Effect of background illumination on the fluorescence yield wave phenomenon in *Thermosynechococcus elongatus* cells. Fluorescence yield changes were detected by applying measuring flashes in logarithmic time sequence (circles), or using logarithmic spacing in the first 100 ms followed by a linearly spaced flash sequence using 0.5 kHz measuring flash repetition rate (solid line). The switch point (100 ms) between the two time sequences is indicated by the arrow. The curves are normalized to the same initial amplitudes.

4. Discussion

Measurement of flash-induced changes in the yield of Chl fluorescence is a widely used method in the investigation of photosynthetic electron transport processes. Relaxation of fluorescence yield, which occurs after the initial, flash-induced increase, has until recently been reported to follow a monotonically decaying time course, and has been interpreted in terms of electron transport events occurring mainly within the PSII complex (see above and in Refs. [1–6]). However, our previous observation of a transient increase of fluorescence yield following its initial decline in intact *Thermosynechococcus* cells [21] and also the appearance of a shoulder in the decay of *Synechocystis* [18] indicated that the kinetics of fluorescence relaxation can be more complex than originally thought, and may provide information about electron transfer processes, which occur outside the PSII complex. In this work we demonstrate for the first time, that under special conditions flash-induced Chl fluorescence relaxation reproducibly exhibits a wave feature that shows a minimum at around few tens of milliseconds, followed by a transient yield increase reaching its maximum at around few seconds after the exciting flash.

Our results demonstrate that PQ mediated electron transfer plays a central role in the wave feature of the fluorescence yield. Scheme 1 summarizes the processes which influence the redox state of the PQ pool in the thylakoid membranes of cyanobacteria. Reduction of the PQ pool occurs via light induced electron transport from PSII, PSI mediated cyclic electron transport, that proceeds directly via Fd or via FNR and the NDH-1 complex [29,34,42–44], as well as by respiratory electron flow via the succinate dehydrogenase (SDH) and NDH-1 complexes. Oxidation of the PQ pool proceeds via a quinol oxidase (Qox) or through the $cytb_6f$ complex, which transfers the electrons to PSI and the terminal cytochrome oxidase (Cox) [45–48] via a water soluble electron carrier (PC, or cyt-c553) [49,50].

The key conditions required for the occurrence of the wave phenomenon in the fluorescence yield relaxation are: (i) Undisturbed light driven linear electron transport from PSII to stromal electron carriers via the $cytb_6f$ complex and PSI. (ii) Highly reduced PQ pool. (iii) Functional electron flow mediated by the NDH-1 complex from highly reduced stromal carriers to the PQ pool. The impacts of these conditions on the fluorescence kinetics are discussed below.

4.1. The role of light driven electron flow from PSII to stromal electron carriers

The wave feature of fluorescence yield relaxation is eliminated by the application of electron transport inhibitors acting at the quinone binding sites of either PSII, or of the $cytb_6f$ complex, as shown by the example of DCMU or DBMIB, respectively. DCMU blocks the binding of mobile PQ molecules at the Q_B binding site of PSII, and inhibits electron transfer from PSII towards the PQ pool. When DCMU binds to the Q_B site PQH_2 cannot be formed, hence equilibration of electrons from the PQ pool back to the Q_B and Q_A acceptors of PSII cannot occur. The backward flow of electrons from the PQ pool to Q_A is very important since this process makes possible to utilize Chl fluorescence, whose yield is modulated by the redox state of Q_A, to monitor the reduction level of the PQ pool. DBMIB inhibits the wave formation of the fluorescence yield by blocking the so called Q_o site of the $cytb_6f$ complex [27] where reoxidation of PQH_2 occurs, thereby preventing reduction of plastocyanin and consequently electron transport towards PSI and the cytochrome oxidase. The wave of fluorescence yield relaxation is also eliminated by the artificial quinone electron acceptor DMBQ, which takes up electrons from PSII, but does not deliver them towards PSI via the $cytb_6f$ complex [28]. The presence of intact electron transport at the level of PSI is also an absolute requirement for the wave feature as demonstrated by the absence of fluorescence yield wave in the *Synechocystis* mutant that lacks the PSI complex.

These data demonstrate that light driven electron transfer from PSII to stromal electron carriers via the $cytb_6f$ and the PSI complexes is a prerequisite of waving fluorescence yield relaxation.

4.2. The role of reduction level of the PQ pool

Although linear electron flow from PSII to stromal electron carriers is clearly required for the appearance of fluorescence yield wave this condition alone is not sufficient for the observed phenomenon. The wave feature of fluorescence yield in dark adapted *Synechocystis* cells appears only under microaerobic conditions when the terminal oxidase activity is impaired due to the lack of its electron acceptor O_2, and consequently the PQ pool becomes significantly reduced in the dark via respiratory electron transport (Scheme 1). This finding leads to the conclusion that increased reduction level of the PQ pool plays an important role in the fluorescence yield wave phenomenon. This idea was confirmed further by detecting waving flash-induced fluorescence decay even under aerobic conditions when the exciting pulse was applied at the top of the post-illumination fluorescence rise. Under these conditions the electron flow from stromal reductants results in a transient reduction of the PQ pool shortly after a preillumination period [31]. It is important to note that in the same preilluminated *Synechocystis* cells the wave phenomenon was completely abolished when the flash was given after 3 min dark adaptation (Fig. 4C), i.e. when the PQ pool became more oxidized by the action of terminal oxidases. The role of the reduction level of the PQ pool in the waving fluorescence yield relaxation was also supported by the observation of this phenomenon in low CO_2-grown *Thermosynechococcus* cells that keep the PQ pool highly reduced in the dark even under aerobic conditions.

These data demonstrate that high reduction level of the PQ pool is crucial for the appearance of the wave phenomenon in the yield of flash-induced fluorescence relaxation. The extensively reduced PQ pool is most likely required for the efficient backflow of electrons from the PQH_2 to Q_A making it possible to monitor the reduction level of the PQ pool by fluorescence yield relaxation.

4.3. The role of the NDH-1 mediated electron flow

Microaerobic conditions not only increase the reduction level of the PQ pool, but enhance also the cyclic electron flow around the PSI complex (see Ref. [43]), which could also be involved in the wave phenomenon of fluorescence relaxation. The essential role of PSI in the fluorescence yield wave as part of the linear electron transport chain has been discussed above. However, PSI is also absolutely required for cyclic electron transport, which can be mediated by mediated directly by Fd and FNR, and indirectly by NDH-1 and succinate dehydrogenase ([29,34,42–44]). Our data showing the absence of fluorescence yield wave in the M55 mutant of *Synechocystis*, that lacks functional NDH-1 complexes [22] demonstrates that NDH-1 is also a critical element of the wave phenomenon. Furthermore, *Synechocystis* and *Thermosynechococcus* cells showed more pronounced fluorescence wave when cultured under low CO_2 conditions that are known to elevate the amount of NDH-1 complexes (see [29]). The role of the NDH-1 complex could be two fold. Being part of the cyclic electron transport chain it is essential for delivering electrons from the acceptor side of PSI back to the PQ pool. On the other hand the NDH-1 complex can also be involved in the generation of highly reduced PQ pool in the dark by mediating respiratory electron flow towards the membrane soluble PQ acceptors. This idea is supported by the impaired respiration of the M55 mutant that lacks functional NDH-1 complexes. In this strain the fluorescence transient lacks not only the “dip” and “bump” features, but the increase of the middle phase, which is assigned to increased reduction of the PQ pool, is also smaller than that observed in the WT cells. Although some cyclic electron flow mediated by the NDH-1-independent antimycin A-sensitive ferredoxin:plastoquinone reductase (FQR) pathway is present in the M55 mutant [34,51] this is insufficient to induce the fluorescence wave phenomenon.

4.4. Wave phenomenon in fluorescence yield relaxation reflects transient changes in the redox state of the PQ pool due to imbalance of linear and NDH-1 mediated electron flow

The wave phenomenon in the fluorescence relaxation kinetics has three main features, which make it different from the usual, monotonous decay. These features are the increased Fo level accompanied with high proportion of the middle phase, and the presence of the dip which is followed by the bump. Our data can be explained in the framework of a model, which postulates that in the presence of highly reduced PQ pool, high level of stromal reductants, as well as functional linear and NDH-1 mediated electron flow illumination by a single turnover flash induces a transient change in the reduction level of the PQ pool, which is transmitted back to Q_A via charge equilibria among the PQH_2, Q_B and Q_A acceptor components and leads to fluctuations in the yield of the fluorescence relaxation transient.

The increased Fo level and the high proportion of the middle phase are direct consequences of highly reduced PQ pool which increases the Q_A^- level in the dark leading to elevated Fo, as well as increases the amount of PSII centers with unoccupied Q_B sites leading to a large middle phase. The explanation of the dip, i.e. the decrease of fluorescence yield close to, or often below the apparent Fo level requires a process that oxidizes the PQ pool to a significant extent at 30–50 ms after the flash. Based on the elimination of the dip by DBMIB and by the lack of

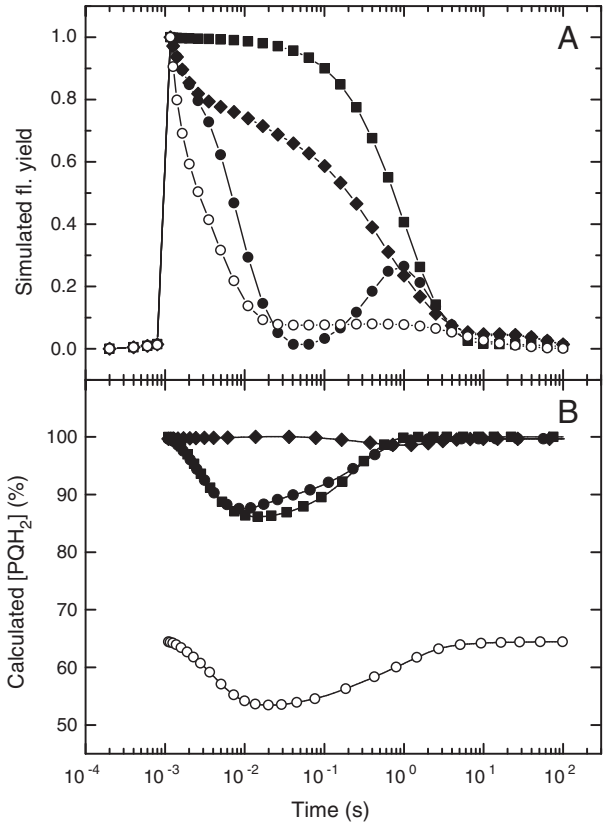

Fig. 9. Simulation of inhibitor effects in *Synechocystis* cells. Flash induced fluorescence transients and the reduction level of the PQ pool was simulated by using an *in silico* model of the electron transport network of *Synechocystis* cells on the basis of Scheme 1 with the rate constants shown in Supplementary Table 2 (the complete list of the included electron transport processes is shown in and Supplementary Table 1). A. Simulated fluorescence transients (A) and PQH_2 concentration (B). Simulations were performed under aerobic conditions in the absence of inhibitors (open circles) and under oxygen deprivation (closed symbols) in the absence of inhibitors (circles) and in the presence of DCMU (squares) or DBMIB (diamonds).

PSI efficient electron withdrawal from the PQ pool by PSI via the cytb$_6$f complex is essential for the appearance of the dip feature. The strong oxidizing effect of the PQ pool by PSI can be explained by the high PSI:PSII ratio which is typical for cyanobacteria [52]. The appearance of the bump, i.e. the transient increase of fluorescence yield in the few tens of ms to the few s time range after the flash, requires a process that feeds electrons back to the PQ pool with a significant time delay after the exciting flash. Based on the lack of the bump in the absence of the NDH-1 complex we suggest that this feature reflects electron flow from reduced stromal components, which is mediated by the NDH-1 complex. The idea of transient oxidation of the PQ pool is supported by the double flash experiment where the change in the reduction state of the PQ pool is reflected by the ratio of the fast and middle phases of fluorescence relaxation after the second flash (Fig. 7).

In order to provide further support for the interpretation of the unusual wave feature of fluorescence relaxation we developed a kinetic model of photosynthetic electron transport, which involves PSII, PSI, cytb$_6$f, NDH-1, PQ, stromal and lumenal electron carriers according to Scheme 1. The involved electron transport processes are listed in Supplementary Table 1, and the rate constants of the individual processes are summarized in Supplementary Table 2. Similar approaches have been used earlier to simulate steady state variable Chl fluorescence induction transients [10,53,54] or CO_2 fixation [55,56]. However, our model describes in detail the interaction of photosynthetic and respiratory electron transport, which are important for the interpretation of the results presented here. As a target of simulation we have chosen the effect of electron transport inhibitors in *Synechocystis* under microaerobic conditions. The data in Fig. 9. show good qualitative agreement between the measured fluorescence transients (presented in Fig. 2) and the simulated changes in the concentration of Q_A^- (Fig. 9A). Furthermore, the simulated changes in the amount of reduced PQ (PQH_2) confirm the idea that the fluorescence yield changes in the dip and bump region of the fluorescence relaxation curves reflect the transient oxidation of the PQ pool. According to the simulation under aerobic conditions the PQ pool is mainly reduced in the dark due to the respiratory electron flow into the PQ pool, which is not compensated by the function of cytochrome and quinol oxidases (Cox and Qox, respectively). Although the light pulse induces a transient decrease in the amount of PQH_2 (Fig. 9B, empty circles), this effect has no detectable influence on the fluorescence transient since the level of reduced PQH_2 is not sufficient to induce significant changes in the amount of Q_A^- via reverse electron flow ($PQH_2/PQ \leftrightarrow Q_B^-/Q_B \leftrightarrow Q_A^-$) (Fig. 9B, empty circles). Under microaerobic conditions, which are simulated by setting the rate constants of the Cox and Qox oxidases to 0 the PQ pool is almost completely reduced before and after the flash and shows a transient oxidation in first 30–50 ms time range after the flash, which is reversed back in the 50 ms–1 s time interval (Fig. 9B, closed circles). This transient oxidation and its recovery corresponds to the development of the dip and bump features of the simulated (Fig. 9A, closed circles) and measured (Fig. 2B open circles), fluorescence yield, and shows also good agreement with the measured change of PQ pool reduction (Fig. 7, C). The transient oxidation of the PQ pool also develops in the presence of DCMU, which is simulated by setting the rate constant of PQ binding to the Q_B site to 0, (Fig. 9B, closed squares). However, in that case backward electron flow from PQH_2 is blocked, therefore the wave feature of the fluorescence transient is eliminated both in the simulated and measured curves (closed squares in Figs. 9A, and 2B, respectively). When the PQH_2 binding to the Qo site of the cytb$_6$f complex is blocked by DBMIB, which is simulated by setting the rate of PQH_2 binding to 0.1, the transient oxidation of the PQ pool is eliminated since PSI cannot extract electrons via cytb$_6$f (Fig. 9B, closed diamonds). Although under these conditions the fluorescence decay is slow due to the low amount of PQ that could deliver electrons from PSII to the PQ pool the wave is eliminated both in the simulated and measured fluorescence curves (closed diamonds in Figs. 9A and 2B, respectively).

We observed wave feature of fluorescence relaxation in various cyanobacterial species (*Synechocystis*, *Thermosynechococcus*, *Synechococcus*) both under aerobic (*Thermosynechococcus*) and microaerobic (*Synechocystis*, *Synechococcus*) conditions. Therefore, the wave feature of fluorescence relaxation appears to represent a general phenomenon under particular experimental conditions. However, in the fluorescence relaxation of *Acaryochloris* cells this wave feature did not appear under the conditions tested in the present work. Although the middle phase of fluorescence decay was increased under microaerobic conditions – indicating an increased reduction level of the PQ pool – a clear dip and bump feature did not develop. Since the redox potential of Q_A/Q_A^- is more positive (−76 mV) in *Acaryochloris* than in *Synechocystis* (−140 mV) [57] the backflow of electrons from PQH_2 to Q_A should not be limiting in *Acaryochloris*. On the other hand the PSI:PSII ratio is significantly smaller in *Acaryochloris* (estimations ranging from 1 [58] to 1.8 [59]) than in *Synechocystis* (ca. 3, [52]). Therefore, electron injection into the PQ pool by PSII and electron withdrawal by PSI during a light pulse should be well balanced in *Acryochloris* preventing or decreasing transient oxidation of the PQ pool, which is a prerequisite of the wave phenomenon.

4.5. Potential applications of the fluorescence yield wave phenomenon

The appearance of wave phenomenon in the relaxation of flash-induced Chl yield increase reflects conditions inside the cells, when highly reduced PQ pool is accompanied with increased activity of the NDH-1 complex. Therefore, characterization of fluorescence wave transients can be a highly useful tool to investigate important features of cyanobacterial electron transport. Some of the obvious targets are: (i) Characterization of the rate of electron transfer from stromal components to the PQ pool. (ii) Clarification of the role of the two forms of FNR [60] in electron delivery to the NDH-1 complex. (iii) Investigation of the role of the recently identified cyanobacterial flavodiiron proteins [6,20,61] in electron delivery processes from PSI and PSII which serve as photoprotective pathways. (iv) Investigation of the role of terminal oxidases in regulating the redox level of the PQ pool under various environmental conditions. These studies require mutants, which are mostly available, and could be performed in forthcoming studies by utilizing the potential of the fluorescence yield wave phenomenon reported here.

Supplementary data to this article can be found online at http://dx.doi.org/10.1016/j.bbabio.2014.01.003.

Acknowledgements

This work was supported by the Hungarian granting agency OTKA (K-101433) and by a grant from TÁMOP-4.2.2.A-11/1/KONV-2012-0047.

References

[1] H.H. Robinson, A. Crofts, Kinetics of the oxidation-reduction reactions of the Photosystem II quinone acceptor complex, and the pathway for deactivation, FEBS Lett. 153 (1983) 221–226.
[2] I. Vass, D. Kirilovsky, A.-L. Etienne, UV-B radiation-induced donor- and acceptor-side modifications of Photosystem II in the cyanobacterium *Synechocystis* sp. PCC 6803, Biochemistry 38 (1999) 12786–12794.
[3] Y. Allahverdiyeva, Zs. Deak, A. Szilárd, B.A. Diner, P.J. Nixon, I. Vass, The function of D1-H332 in Photosystem II electron transport studied by thermoluminescence and chlorophyll fluorescence in site-directed mutants of *Synechocystis* 6803, Eur. J. Biochem. 271 (2004) 3523–3532.
[4] K. Cser, B.A. Diner, P.J. Nixon, I. Vass, The role of D1-Ala344 in charge stabilization and recombination in Photosystem II, Photochem. Photobiol. Sci. 4 (2005) 1049–1054.
[5] K. Cser, Z. Deák, A. Telfer, J. Barber, I. Vass, Energetics of Photosystem II charge recombination in *Acaryochloris marina* studied by thermoluminescence and flash-induced chlorophyll fluorescence measurements, Photosynth. Res. 98 (2008) 131–140.
[6] P. Zhang, M. Eisenhut, A.-M. Brandt, D. Carmel, H.M. Silén, I. Vass, Y. Allahverdiyeva, T.A. Salminen, E.-M. Aro, Operon *flv4-flv2* provides cyanobacterial Photosystem II with flexibility of electron transfer, Plant Cell 24 (2012) 1952–1971.

[7] A. Volgusheva, S. Styring, F. Mamedov, Increased photosystem II stability promotes H_2 production in sulfur-deprived *Chlamydomonas reinhardtii*, Proc. Natl. Acad. Sci. U. S. A. 110 (2013) 7223–7228.
[8] G.H. Krause, Chlorophyll fluorescence and photosynthesis: the basics, Annu. Rev. Plant Physiol. 42 (1991) 313–349.
[9] H. Dau, Molecular mechanisms and quantitative models of variable Photosystem II fluorescence, Photochem. Photobiol. 60 (1994) 1–23.
[10] D. Lazar, Review chlorophyll *a* fluorescence induction, Biochim. Biophys. Acta 1412 (1999) 1–28.
[11] A.R. Crofts, C.A. Wraight, The electrochemical domain of photosynthesis, Biochim. Biophys. Acta 726 (1983) 149–185.
[12] A. Crofts, I. Baroli, D.M. Kramer, S. Taoka, Kinetics of electron transfer between Q_A and Q_B in wild type and herbicide-resistant mutants of *Chlamydomonas reinhardtii*, Z. Naturforsch. 48c (1993) 259–266.
[13] G. Renger, H.-J. Eckert, A. Bergmann, J. Bernarding, B. Liu, A. Napiwotzki, F. Reifarth, H.-J. Eichler, Fluorescence and spectroscopic studies of exciton trapping and electron transfer in Photosystem II of higher plants, Aust. J. Plant Physiol. 22 (1995) 167–181.
[14] H.-A. Chu, A.P. Nguyen, R.J. Debus, Site-directed Photosystem II mutants with perturbed oxygen-evolving properties. 1. Instability or inefficient assembly of the manganese cluster *in vivo*, Biochemistry 33 (1994) 6137–6149.
[15] J. Kargul, K. Maghlaoui, J.W. Murray, Zs. Deak, A. Boussac, A.W. Rutherford, I. Vass, J. Barber, Purification, crystallization and X-ray diffraction analyses of the *T. elongatus* PSII core dimer with strontium replacing calcium in the oxygen-evolving complex, Biochim. Biophys. Acta 1767 (2007) 404–413.
[16] S. Rantamäki, E. Tyystjarvi, Analysis of S_2Q_A charge recombination with the Arrhenius, Eyring and Marcus theories, J. Photochem. Photobiol. B 104 (2011) 292–300.
[17] Y. Zhang, S. Ding, Q. Lu, Z. Yang, X. Wen, L. Zhang, C. Lu, Characterization of photosystem II in transgenic tobacco plants with decreased iron superoxide dismutase, Biochim. Biophys. Acta 1807 (2011) 391–403.
[18] Q.J. Wang, A. Singh, H. Li, L. Nedbal, L.A. Sherman, Govindjee, J. Whitmarsh, Net light-induced oxygen evolution in photosystem I deletion mutants of the cyanobacterium *Synechocystis* sp. PCC 6803, Biochim. Biophys. Acta 1817 (2012) 792–801.
[19] I. Hasni, S. Hamdani, R. Carpentier, Destabilization of the oxygen evolving complex of photosystem II by Al^{3+}, Photochem. Photobiol. 89 (2013) 1135–1142.
[20] Y. Allahverdiyeva, H. Mustila, M. Ermakova, L. Bersanini, P. Richaud, G. Ajlani, N. Battchikova, L. Cournac, E.-M. Aro, Flavodiiron proteins Flv1 and Flv3 enable cyanobacterial growth and photosynthesis under fluctuating light, Proc. Natl. Acad. Sci. U. S. A. 110 (2013) 4111–4116.
[21] Z. Deák, I. Vass, Oscillating yield of flash-induced chlorophyll fluorescence decay in intact cells of *Thermosynechococcus Elongatus*, Energy From the Sun, 14th International Congress on Photosynthesis, Springer, 2008.
[22] T. Ogawa, A gene homologous to the subunit-2 gene of NADH dehydrogenase is essential to inorganic carbon transport of *Synechocystis* PCC6803, Proc. Natl. Acad. Sci. U. S. A. 88 (1991) 4275–4279.
[23] G. Shen, S. Boussiba, W.F.J. Vermaas, *Synechocystis* sp PCC 6803 and phycobilisome function strains lacking photosystem I, Plant Cell 5 (1993) 1853–1863.
[24] M. Trtilek, D.M. Kramer, M. Koblizek, Dual-modulation LED kinetic fluorometer, J. Lumin. 72–74 (1997) 597–599.
[25] A. Joliot, P. Joliot, Etude cinétique de la réaction photochimique libérant l'oxygéne au cours de la photosynthése, C. R. Acad. Sci. 258 (1964) 4622–4625.
[26] K. Asada, U. Heber, U. Schreiber, Electron flow to the intersystem chain from stromal components and cyclic electron flow in maize chloroplasts, as detected in intact leaves by monitoring redox change of P700 and chlorophyll fluorescence, Plant Cell Physiol. 34 (1993) 39–50.
[27] G. Kurisu, H. Zhang, J.L. Smith, W.A. Cramer, Structure of the cytochrome b_6f complex of oxygenic photosynthesis: tuning the cavity, Science 302 (2003) 1009–1014.
[28] S. Izawa, Acceptors and donors for chloroplast electron transport, Methods Enzymol. 69 (1980) 413–434.
[29] N. Battchikova, M. Eisenhut, E.-M. Aro, Cyanobacterial NDH-1 complexes: novel insights and remaining puzzles, Biochim. Biophys. Acta 1807 (2011) 935–944.
[30] H. Mi, T. Endo, U. Schreiber, T. Ogawa, K. Asada, Electron donation from cyclic and respiratory flows to the photosynthetic intersystem chain is mediated by pyridine nucleotide dehydrogenase in the cyanobacterium *Synechocystis* PCC 6803, Plant Cell Physiol. 33 (1992) 1233–1237.
[31] J. Mano, C. Miyake, U. Schreiber, K. Asada, Photoactivation of the electron flow from NADPH to plastoquinone in spinach chloroplasts, Plant Cell Physiol. 36 (1995) 1589–1598.
[32] H. Mi, T. Endo, T. Ogawa, K. Asada, Thylakoid membrane-bound, NADPH-specific pyridine nucleotide dehydrogenase complex mediates cyclic electron transport in the cyanobacterium *Synechocystis* sp. PCC 6803, Plant Cell Physiol. 36 (1995) 661–668.
[33] T. Shikanai, T. Endo, T. Hashimoto, Y. Yamada, K. Asada, A. Yokota, Directed disruption of the tobacco *ndhB* gene impairs cyclic electron flow around Photosystem I, Proc. Natl. Acad. Sci. U. S. A. 95 (1998) 9705–9709.
[34] Y. Munekage, M. Hashimoto, C. Miyake, K.-I. Tomizawa, T. Endo, M. Tasaka, T. Shikanai, Cyclic electron flow around Photosystem I is essential for photosynthesis, Nature 429 (2004) 579–582.
[35] S. Sirpiö, Y. Allahverdiyeva, M. Holmström, A. Khrouchtchova, A. Haldrup, N. Battchikova, E.-M. Aro, Novel nuclear-encoded subunits of the chloroplast NAD(P)H dehydrogenase complex, J. Biol. Chem. 284 (2009) 905–912.
[36] E. Gotoh, M. Matsumoto, K. Ogawa, Y. Kobayashi, M. Tsuyama, A qualitative analysis of the regulation of cyclic electron flow around photosystem I from the post-illumination chlorophyll fluorescence transient in Arabidopsis: a new platform for the in vivo investigation of the chloroplast redox state, Photosynth. Res. 103 (2010) 123.
[37] W. Ma, H. Mi, Expression and activity of type 1 NAD(P)H dehydrogenase at different growth phases of the cyanobacterium, *Synechocystis* PCC 6803, Physiol. Plant. 125 (2005) 135–140.
[38] Y. Deng, J. Ye, H. Mi, Effects of low CO_2 on NAD(P)H dehydrogenase, a mediator of cyclic electron transport around photosystem I in the cyanobacterium *Synechocystis* PCC6803, Plant Cell Physiol. 44 (2003) 534–540.
[39] W. Ma, Y. Deng, T. Ogawa, H. Mi, Active NDH-1 complexes from the cyanobacterium *Synechocystis* sp. strain PCC 6803, Plant Cell Physiol. 47 (2006) 1432–1436.
[40] H. Mi, Y. Deng, Y. Tanaka, T. Hibino, T. Takabe, Photo-induction of an NADPH dehydrogenase which functions as a mediator of electron transport to the intersystem chain in the cyanobacterium *Synechocystis* PCC6803, Photosynth. Res. 70 (2001) 167–173.
[41] E. Miskiewicz, A.G. Ivanov, N.P.A. Huner, Stoichiometry of the photosynthetic apparatus and phycobilisome structure of the cyanobacterium *Plectonema boryanum* UTEX 485 are regulated by both light and temperature, Plant Physiol. 130 (2002) 1414–1425.
[42] T. Shikanai, Cyclic electron transport around Photosystem I: Genetic approaches, Annu. Rev. Plant Biol. 58 (2007) 199–217.
[43] J. Alric, Cyclic electron flow around photosystem I in unicellular green algae, Photosynth. Res. 106 (2010) 47–56.
[44] G.N. Johnson, Physiology of PSI cyclic electron transport in higher plants, Biochim. Biophys. Acta 1807 (2011) 384–389.
[45] D. Pils, G. Schmetterer, Characterization of three bioenergetically active respiratory terminal oxidases in the cyanobacterium *Synechocystis* sp. strain PCC 6803, FEMS Microbiol. Lett. 203 (2001) 217–222.
[46] S. Berry, D. Schneider, W.F.J. Vermaas, M. Rögner, Electron transport routes in whole cells of *Synechocystis* sp. Strain PCC 6803: the role of the cytochrome *bd*-type oxidase, Biochemistry 41 (2002) 3422–3429.
[47] F. Gutthann, M. Egert, A. Marques, J. Appel, Inhibition of respiration and nitrate assimilation enhances photohydrogen evolution under low oxygen concentrations in *Synechocystis* sp. PCC 6803, Biochim. Biophys. Acta 1767 (2007) 161–169.
[48] M. Schultze, B. Forberich, S. Rexroth, N.G. Dyczmons, M. Roegner, J. Appel, Localization of cytochrome b_6f complexes implies an incomplete respiratory chain in cytoplasmic membranes of the cyanobacterium *Synechocystis* sp. PCC 6803, Biochim. Biophys. Acta 1787 (2009) 1479–1485.
[49] K.K. Ho, D.W. Krogmann, Electron donors to P700 in cyanobacteria and algae an instance of unusual genetic variability, Biochim. Biophys. Acta 766 (1984) 310–316.
[50] P.M. Wood, Interchangeable copper and iron proteins in algal photosynthesis.Studies on plastocyanin and cytochrome c-552 in Chlamydomonas, Eur. J. Biochem. 87 (1978) 9–19.
[51] N. Yeremenko, R. Jeanjean, P. Prommeenate, V. Krasikov, P.J. Nixon, W.F.J. Vermaas, M. Havaux, H.C.P. Matthijs, Open reading frame *ssr2016* is required for antimycin A-sensitive Photosystem I-driven cyclic electron flow in the cyanobacterium *Synechocystis* sp. PCC 6803, Plant Cell Physiol. 46 (2005) 1433–1436.
[52] K. Aizawa, T. Shimizu, T. Hiyama, K. Satoh, Y. Nakamura, Y. Fujita, Changes in composition of membrane-proteins accompanying the regulation of PS-I/PS-II stoichiometry observed with *Synechocystis* PCC 6803, Photosynth. Res. 32 (1992) 131–138.
[53] X.G. Zhu, Govindjee, N.R. Baker, E. deSturler, D.R. Ort, S.P. Long, Chlorophyll *a* fluorescence induction kinetics in leaves predicted from a model describing each discrete step of excitation energy and electron transfer associated with photosystem II, Planta 223 (2005) 114–133.
[54] C.-P. Xin, J. Yang, X.-G. Zhu, A model of chlorophyll a fluorescence induction kinetics with explicit description of structural constraints of individual photosystem II units, Photosynth. Res. 117 (2013) 339–354.
[55] A. Laisk, H. Eichelmann, V. Oja, C_3 photosynthesis *in silico*, Photosynth. Res. 90 (2006) 45–66.
[56] X.-G. Zhu, Y. Wang, D.R. Ort, S.P. Long, e-photosynthesis: a comprehensive dynamic mechanistic model of C3 photosynthesis: from light capture to sucrose synthesis, Plant Cell Environ. 36 (2013) 1711–1727.
[57] S.I. Allakhverdiev, T. Tsuchiya, K. Watabe, A. Kojima, D.A. Los, T. Tomo, V.V. Klimov, M. Mimuro, Redox potentials of primary electron acceptor quinone molecule $(Q_A)^-$ and conserved energetics of photosystem II in cyanobacteria with chlorophyll *a* and chlorophyll *d*, Proc. Natl. Acad. Sci. U. S. A. 108 (2011) 8054–8058.
[58] M. Mimuro, S. Akimoto, T. Gotoh, M. Yokono, M. Akiyama, T. Tsuchiya, H. Miyashita, M. Kobayachi, I. Yamazaki, Identification of the primary electron donor in PS II of the Chl *d*-dominated cyanobacterium *Acaryochloris marina*, FEBS Lett. 556 (2004) 95–98.
[59] S. Itoh, H. Mino, K. Itoh, T. Shigenaga, T. Uzumaki, M. Iwaki, Function of chlorophyll *d* in reaction centers of Photosystems I and II of the oxygenic photosynthesis of *Acaryochloris marina*, Biochemistry 46 (2007) 12473–12481.
[60] J.-C. Thomas, B. Ughy, B. Lagoutte, G. Ajlani, A second isoform of the ferredoxin: NADP oxidoreductase generated by an in-frame initiation of translation, Proc. Natl. Acad. Sci. U. S. A. 103 (2006) 18368–18373.
[61] P. Zhang, Y. Allahverdiyeva, M. Eisenhut, E.-M. Aro, Flavodiiron proteins in oxygenic photosynthetic organisms: photoprotection of photosystem II by Flv2 and Flv4 in *Synechocystis* sp. PCC 6803, Plos One 4 (2009) e5331.
[62] G. Guedeney, S. Corneille, S. Cuine, G. Peltier, Evidence for an association of *ndh* B, *ndh* J gene products and ferredoxin-NADP-reductase as components of a chloroplastic NAD(P)H dehydrogenase complex, FEBS Lett. 378 (1996) 277–280.